

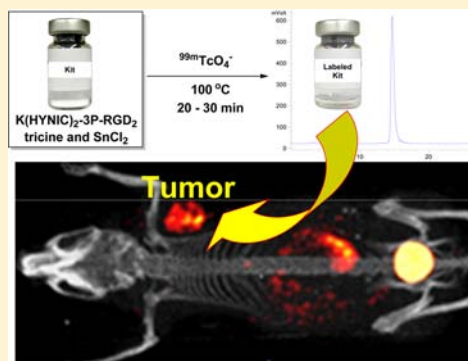
Evaluation of K(HYNIC)₂ as a Bifunctional Chelator for ^{99m}Tc-Labeling of Small Biomolecules

Shundong Ji, Yang Zhou, Guoqiang Shao, and Shuang Liu*

School of Health Sciences, Purdue University, West Lafayette, Indiana, United States

Supporting Information

ABSTRACT: This study sought to evaluate K(HYNIC)₂ (K = lysine and HYNIC = 6-hydrazinonicotinyl) as a bifunctional chelator for ^{99m}Tc-labeling of biomolecule. In this study, four K(HYNIC)₂-conjugated cyclic RGD peptides, K(HYNIC)₂-RGD₂ (RGD₂ = E[c(RGDfK)]₂), K(HYNIC)₂-3G-RGD₂ (3G-RGD₂ = Gly-Gly-Gly-E[Gly-Gly-Gly-c(RGDfK)]₂), K(HYNIC)₂-2P-RGD₂ (2P-RGD₂ = E[PEG₄-c(RGDfK)]₂), and PEG₄ = 15-amino-4,7,10,13-tetraoxapentadecanoic acid), and K(HYNIC)₂-3P-RGD₂ (3P-RGD₂ = PEG₄-E[PEG₄-c(RGDfK)]₂) were prepared, and evaluated for their integrin $\alpha_v\beta_3$ binding affinity. IC₅₀ values were determined to be 47 ± 2, 35 ± 2, 37 ± 2, 85 ± 2, and 422 ± 15 nM for K(HYNIC)₂-2P-RGD₂, K(HYNIC)₂-3P-RGD₂, K(HYNIC)₂-3G-RGD₂, K(HYNIC)₂-RGD₂, and c(RGDyK), respectively, against ¹²⁵I-echistatin bound to U87MG cells. Macrocytic complexes [^{99m}Tc(K(HYNIC)₂-RGD₂)(tricine)] (1), [^{99m}Tc(K(HYNIC)₂-3G-RGD₂)(tricine)] (2), [^{99m}Tc(K(HYNIC)₂-2P-RGD₂)(tricine)] (3), and [^{99m}Tc(K(HYNIC)₂-3P-RGD₂)(tricine)] (4) were prepared, and evaluated in athymic nude mice bearing U87MG glioma xenografts for their tumor targeting capability and biodistribution. It was found that 1–4 all had high solution stability and more than two isomers, as evidenced by the presence of multiple radiometric peaks in their radio-HPLC chromatograms. The tumor uptake of 1–4 was 3.78 ± 0.81, 7.46 ± 1.68, 9.74 ± 1.65, and 8.59 ± 1.52%ID/g, respectively, which was completely consistent with trend of integrin $\alpha_v\beta_3$ binding affinity for cyclic RGD peptides. Replacing [^{99m}Tc(HYNIC)(tricine)(TPPTS)] (TPPTS = trisodium triphenylphosphine-3,3',3''-trisulfonate) with [^{99m}Tc(K(HYNIC)₂)(tricine)] had little impact on radiotracer tumor uptake; but it had significant effect on the uptake of radiotracer in kidneys, lungs, and spleen. The tumor was clearly visualized by SPECT/CT with excellent contrast in a glioma-bearing mouse administered with 4. K(HYNIC)₂ would be particularly useful for ^{99m}Tc-labeling of small biomolecules with one or more disulfide linkages.



INTRODUCTION

Since 6-hydrazinonicotinamide (HYNIC) was first reported as a bifunctional coupling agent (BFC) for ^{99m}Tc-labeling of polyclonal IgG,^{1,2} it has been widely used to label antibodies and other biomolecules (BM) with ^{99m}Tc.^{3–18} We have been using a ternary ligand system (Figure 1A: HYNIC, tricine, and TPPTS (trisodium triphenylphosphine-3,3',3''-trisulfonate)) to prepare ^{99m}Tc-labeled chemotactic peptides and leukotriene B₄ (LTB₄) receptor antagonists for imaging infection and inflammation,^{19,20} glycoprotein IIb/IIIa receptor antagonists for thrombosis imaging,²¹ and integrin $\alpha_v\beta_3$ receptor antagonists for tumor imaging.^{22–25} Ternary ligand complexes [^{99m}Tc(HYNIC-BM)(tricine)(TPPTS)] (Figure 1A: BM = peptide and nonpeptide receptor ligands) were prepared with high specific activity, and had very high solution stability.^{19–25} Their composition has been determined to be 1:1:1:1 for Tc:HYNIC:tricine:TPPTS through a series of mixed ligand experiments,²⁶ and further confirmed by LC-MS at the tracer (^{99m}Tc) and macroscopic (⁹⁹Tc) levels.²⁷ The utility of HYNIC has been reviewed extensively.^{28–30}

Previously, we reported HYNIC-K(NIC) (ω -nicotinyl-2-(6-hydrazinonicotinyl)lysine) as a BFC for ^{99m}Tc-labeling of biomolecules, and found that HYNIC-K(NIC) was able to

form a macrocyclic chelate [^{99m}Tc(HYNIC-K(NIC))(tricine)] (Figure 1B) with high solution stability.³¹ We also found that replacing [^{99m}Tc(HYNIC)(tricine)(TPPTS)] with [^{99m}Tc(HYNIC-K(NIC))(tricine)] resulted in less uptake in kidneys and lungs for ^{99m}Tc radiotracers.³² These promising results inspired us to evaluate K(HYNIC)₂ as a BFC for ^{99m}Tc-labeling of cyclic RGD peptides. We reasoned that K(HYNIC)₂ and HYNIC-K(NIC) would form macrocyclic ^{99m}Tc complexes with a similar structure except that one of two HYNIC groups in K(HYNIC)₂ might be bidentate (Figure 1C). Since SnCl₂ is used to reduce ^{99m}TcO₄[−], there is no need for TPPTS as the reducing agent for ^{99m}TcO₄[−] and a coligand to stabilize the ^{99m}Tc-HYNIC core. This is particularly important for ^{99m}Tc-labeling of small biomolecules with one or more disulfide linkages, which could be readily reduced by TPPTS at elevated temperatures.

As a continuation of our interest in radiolabeled cyclic RGD peptides as integrin $\alpha_v\beta_3$ -targeted radiotracers for tumor imaging,^{32–41} we have prepared four K(HYNIC)₂-conjugated

Received: December 27, 2012

Revised: March 21, 2013

Published: March 25, 2013



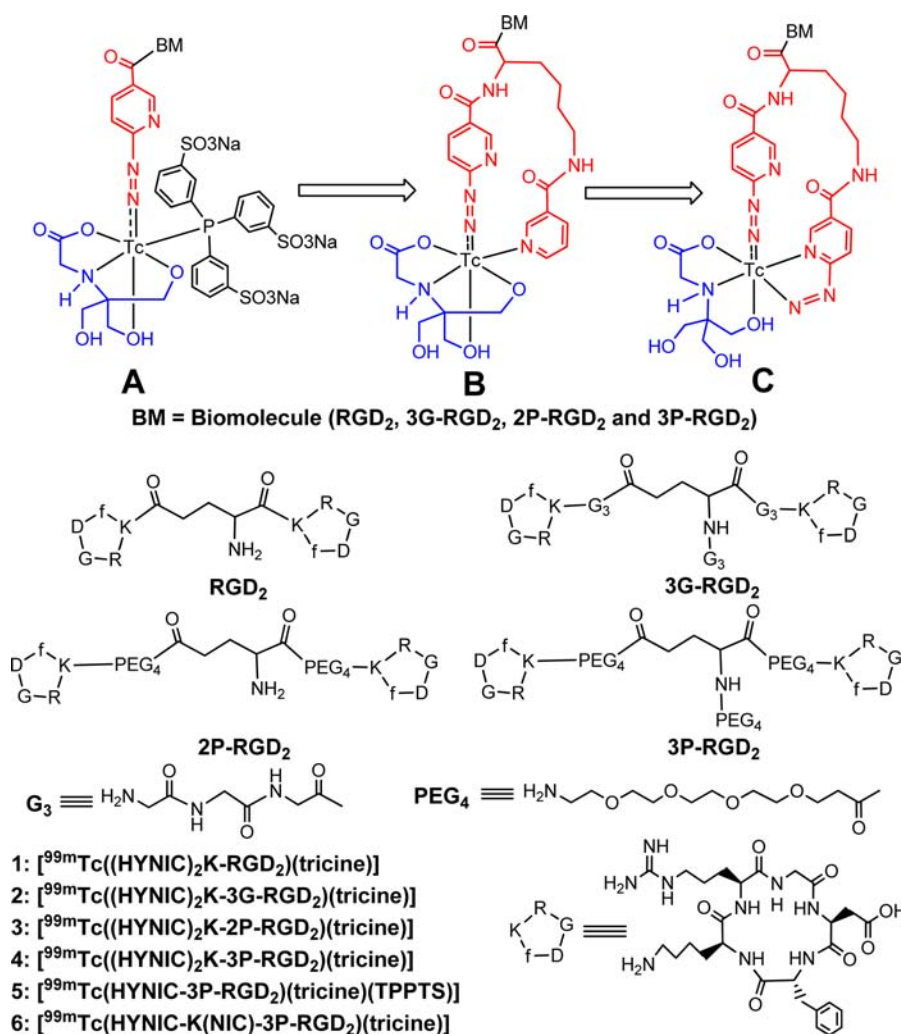


Figure 1. Structure of cyclic RGD peptide dimers and their ^{99m}Tc complexes. Structure A represents the ternary ligand system, in which tricine and TPPTS are used as coligands to stabilize the ^{99m}Tc -HYNIC core. Structure B represents the HYNIC-K(NIC) chelating system with tricine as coligand to complete the octahedral coordination sphere of technetium. In this way, the highly charged TPPTS is eliminated. Structure C represents the (HYNIC) $_2$ K chelating system, in which one HYNIC is monodentate and the other is bidentate while tricine is tridentate. The biomolecule (BM) is a cyclic RGD peptide or nonpeptide receptor ligand. The small letter “F” in cyclic peptides represents D-phenylalanine.

cyclic RGD peptides: K(HYNIC)₂-RGD₂ (RGD₂ = E[ϵ -(RGDfK)]₂), K(HYNIC)₂-3G-RGD₂ (3G-RGD₂ = Gly-Gly-Gly-E[Gly-Gly-Gly-c(RGDfK)]₂), K(HYNIC)₂-2P-RGD₂ (2P-RGD₂ = E[PEG₄-c(RGDfK)]₂), and PEG₄ = 15-amino-4,7,10,13-tetraoxapentadecanoic acid), and K(HYNIC)₂-3P-RGD₂ (3P-RGD₂ = PEG₄-E[PEG₄-c(RGDfK)]₂). An in vitro whole-cell assay was used to determine their integrin $\alpha_v\beta_3$ binding affinity against ¹²⁵I-echistatin bound to U87MG human glioma cells. We also prepared macrocyclic complexes [^{99m}Tc-(K(HYNIC)₂-RGD₂)(tricine)] (1), [^{99m}Tc(K(HYNIC)₂-3G-RGD₂)(tricine)] (2), [^{99m}Tc(K(HYNIC)₂-2P-RGD₂)(tricine)] (3) and [^{99m}Tc(K(HYNIC)₂-3P-RGD₂)(tricine)] (4), and evaluated them in the athymic nude mice bearing U87MG glioma xenografts for their tumor-targeting capability and biodistribution characteristics. The objective of this study is to explore the potential of K(HYNIC)₂ as a BFC, and compare the three chelating systems (Figure 1: A–C) with respect to the isomerism and biodistribution of the ^{99m}Tc-labeled of cyclic RGD peptides (Figure 1: 1–6).

■ EXPERIMENTAL SECTION

Materials and Instruments. Chemicals and solvents were purchased from Sigma-Aldrich (St. Louis, MO). Cyclic peptides, E[c(RGDfk)]₂ (RGD₂), G₃-E[G₃-c(RGDfk)]₂ (3G-RGD₂), E[PEG₄-c(RGDfk)]₂ (2P-RGD₂), and PEG₄-E[PEG₄-c(RGDfk)]₂ (3P-RGD₂) were obtained from the Peptides International, Inc. (Louisville, KY). Sodium succinimidyl 6-(2-(2-sulfonatobenzaldehyde)hydrazono)nicotinate (HYNIC-OSu) was prepared according to literature method.⁴² [^{99m}Tc-(HYNIC-3P-RGD₂)(tricine)(TPPTS)] (5) and [^{99m}Tc-(HYNIC-K(NIC)-3P-RGD₂)(tricine)] (6) were prepared using the procedures described in our previous reports.^{32,33} Na^{99m}TcO₄ was obtained from Cardinal HealthCare (Chicago, IL). Electrospray ionization (ESI) mass spectra were collected on a Finnigan LCQ mass spectrometer, School of Pharmacy, Purdue University.

HPLC Methods. The semiprep HPLC method (Method 1) used a LabAlliance HPLC system (Scientific Systems, Inc., State College, PA) equipped with a UV/vis detector ($\lambda = 254$ nm) and Zorbax C₁₈ column (9.4 mm \times 250 mm, 100 Å pore size; Agilent Technologies, Santa Clara, CA). The flow rate was

2.5 mL/min with a gradient mobile phase going from 90% A (0.1% TFA in water) and 10% B (0.1% TFA in acetonitrile) at 0 min to 30% B at 5 min, and 50% B at 18 min. The radio-HPLC (Method 2) used the LabAlliance HPLC system equipped with a β -ram IN/US detector (Tampa, FL) and Zorbax C₁₈ column (4.6 mm \times 250 mm, 300 Å pore size; Agilent Technologies, Santa Clara, CA). The flow rate was 1 mL/min. The gradient mobile phase started with 90% A (25 mM NH₄OAc, pH = 6.8) and 10% B (acetonitrile) to 85% A and 15% B at 5 min, followed by a gradient mobile phase going from 15% B at 5 min to 20% B at 20 min and to 60% B at 25 min.

Lys(Boc)₂-E[c(RGDfK)]₂ (K(Boc)₂-RGD₂). K(Boc)₂-OSu (8.8 mg, 20 μ mol) and RGD₂ (13.2 mg, 10 μ mol) were dissolved in DMF (2 mL). After addition of DIEA (50 μ mol), the reaction mixture was stirred at room temperature for 5 h. The reaction was terminated by adding 2 mL of NH₄OAc buffer (100 mM, pH = 7.0), and the product was separated by semiprep HPLC (Method 1). The fractions at 15.3 min were collected. Lyophilization of the collected fractions afforded K(Boc)₂-RGD₂. The yield was 11 mg (~67%). ESI-MS: m/z = 1646.5 for [M + H]⁺ (M = 1645.86 calcd. for [C₇₅H₁₁₅N₂₁O₂₁]).

Lys-E[c(RGDfK)]₂ (K-RGD₂). K(Boc)₂-RGD₂ (3.3 mg, 2 μ mol) was dissolved in anhydrous trifluoroacetic acid (TFA, 1 mL). After stirring at room temperature for 5–10 min, excess TFA was removed on a rotary evaporator. The residue was dissolved in 2 mL of water. The product was isolated by semiprep HPLC (Method 1). Fractions at 11.4 min were collected and combined. Lyophilization of the resulting solution afforded the expected product K-RGD₂ as its TFA salt. The yield was 2.1 mg (~72%). ESI-MS: m/z = 1446.8 for [M + H]⁺ (M = 1445.75 calcd. for [C₆₅H₉₉N₂₁O₁₇]).

Lys(HYNIC)₂-E[c(RGDfK)]₂ (K(HYNIC)₂-RGD₂). HYNIC-OSu (4.6 mg, 10 μ mol) and K-RGD₂ (2.9 mg, 2.0 μ mol) were dissolved in DMF (1 mL). After addition of excess DIEA (40 μ mol), the reaction mixture was stirred at room temperature for 7 days. Upon addition of 2 mL ammonium acetate buffer (100 mM, pH = 7.0) to terminate the reaction, the product was separated by semiprep HPLC method (Method 1). The fractions at 17.8 min were collected. Lyophilization of the collected fractions afforded K-(HYNIC)₂-RGD₂. The yield was 1.5 mg (~37%). ESI-MS: m/z = 2053.3 for [M + H]⁺ and 1027.5 for [M + H]²⁺ (M = 2051.82 calcd. for [C₉₁H₁₁₇N₂₇O₂₅S₂]).

Lys(Boc)₂-G₃-E[G₃-c(RGDfK)]₂ (K(Boc)₂-3G-RGD₂). K(Boc)₂-OSu (13.2 mg, 30 μ mol) and 3G-RGD₂ (18.3 mg, 10 μ mol) were dissolved in DMF (2 mL). After adding excess DIEA (50 μ mol), the reaction mixture was stirred at room temperature for 5 h. After addition of 2 mL water, the pH was then adjusted to 4.0 with TFA. The product was isolated from the mixture using the same HPLC method used for K(Boc)₂-RGD₂. The fractions at 14.5 min were collected. Lyophilization of the collected fractions afforded K(Boc)₂-3G-RGD₂. The yield was 10.4 mg (48%). ESI-MS: m/z = 2159.9 for [M + H]⁺ (M = 2159.05 calcd. for [C₉₃H₁₄₂N₃₀O₃₀]).

Lys-G₃-E[G₃-c(RGDfK)]₂ (K-3G-RGD₂). K(Boc)₂-3G-RGD₂ (4.3 mg, 2 μ mol) was dissolved in anhydrous trifluoroacetic acid (TFA, 1 mL). After stirring at room temperature for 5–10 min, excess TFA was removed on a rotary evaporator. The residue was dissolved in 2 mL of water. The product was isolated by semiprep HPLC (Method 1). The fractions at 9.5 min were collected and combined. Lyophilization of the

combined fractions afforded the expected product K-3G-RGD₂ as its TFA salt. The yield was 3.5 mg (~89%). ESI-MS: m/z = 2160.6 for [M + H]⁺ (M = 1958.95 calcd. for [C₈₃H₁₂₆N₃₀O₂₆]).

Lys(HYNIC)₂-G₃-E[G₃-c(RGDfK)]₂ (K(HYNIC)₂-3G-RGD₂). HYNIC-OSu (4.6 mg, 10 μ mol) and K-3G-RGD₂ (1.96 mg, 1.0 μ mol) were dissolved in anhydrous DMF (1 mL). After addition of excess (50 μ mol), the reaction mixture was stirred at room temperature for 7 days. Upon addition of 2 mL NH₄OAc buffer (100 mM, pH = 7.0), the product was separated from the mixture using the same HPLC method for K(HYNIC)₂-RGD₂. The fractions at 15.6 min were collected and combined. Lyophilization of the resulting solution afforded K(HYNIC)₂-3G-RGD₂. The yield was 1.2 mg (47%). ESI-MS: m/z = 2567.8 for [M + H]⁺ and 1582.2 for [M + H]²⁺ (M = 2565.01 calcd. for [C₁₀₉H₁₄₄N₃₆O₃₄S₂]).

Lys(Boc)₂-E[PEG₄-c(RGDfK)]₂ (K(Boc)₂-2P-RGD₂). K(Boc)₂-OSu (13.2 mg, 30 μ mol) and 2P-RGD₂ (19.6 mg, 10 μ mol) were dissolved in DMF (2 mL). After addition of excess DIEA (50 μ mol), the reaction mixture was stirred at room temperature for 5 h. Upon addition of 2 mL NH₄OAc buffer (100 mM, pH = 7.0), the product was separated using the same method for K(Boc)₂-RGD₂. The fractions at 14.7 min were collected. Lyophilization of collected fractions afforded K-(Boc)₂-2P-RGD₂. The yield was 13.4 mg (~63%). ESI-MS: m/z = 2141.0 for [M + H]⁺ (M = 2140.14 calcd. for [C₉₇H₁₅₇N₂₃O₃₁]).

Lys-E[PEG₄-c(RGDfK)]₂ (K-2P-RGD₂). K(Boc)₂-2P-RGD₂ (2.14 mg, 1 μ mol) was dissolved in anhydrous trifluoroacetic acid (TFA, 1 mL). After stirring at room temperature for 5–10 min, excess TFA was removed on a rotary evaporator. The residue was dissolved in 2 mL of water. The product was isolated by semiprep HPLC (Method 1). Fractions at 11.3 min were collected. Lyophilization of the collected fractions afforded the expected product K-2P-RGD₂. ESI-MS: m/z = 1941.14 for [M + H]⁺ (M = 1940.04 calcd. for [C₈₇H₁₄₁N₂₃O₂₇]).

Lys(HYNIC)₂-E[PEG₄-c(RGDfK)]₂ (K(HYNIC)₂-2P-RGD₂). HYNIC-OSu (4.6 mg, 10 μ mol) and K-2P-RGD₂ (1.9 mg, 1.0 μ mol) were dissolved in DMF (1 mL). After addition of DIEA (50 μ mol), the reaction mixture was stirred at room temperature for 7 days. The reaction was terminated by adding 2 mL of NH₄OAc buffer (100 mM, pH = 7.0), the product was separated using the same HPLC method for K(HYNIC)₂-RGD₂. The fractions at 20.4 min were collected. Lyophilization of the collected fractions afforded the expected product K(HYNIC)₂-2P-RGD₂. The yield was 1.7 mg (~67%). ESI-MS: m/z = 2546.9 for [M + H]⁺ and 1274.4 for [M + H]²⁺ (M = 2546.10 calcd. for [C₁₁₃H₁₅₉N₂₉O₃₅S₂]).

Lys(Boc)₂-PEG₄-E[PEG₄-c(RGDfK)]₂ (K(Boc)₂-3P-RGD₂). K(Boc)₂-OSu (13.2 mg, 30 μ mol) and 3P-RGD₂ (20.7 mg, 10 μ mol) were dissolved in DMF (2 mL). After addition of excess DIEA (50 μ mol), the reaction mixture was stirred at room temperature for 5 h. The product was separated using the same HPLC method for K(Boc)₂-RGD₂. The fractions at 15.5 min were collected. Lyophilization of collected fractions afforded K(Boc)₂-3P-RGD₂. The yield was 14.6 mg (~61%). ESI-MS: m/z = 2388.2 for [M + H]⁺ (M = 2387.28 calcd. for [C₁₀₈H₁₇₈N₂₄O₃₆]).

Lys-PEG₄-E[PEG₄-c(RGDfK)]₂ (K-3P-RGD₂). K(Boc)₂-3P-RGD₂ (2.4 mg, 1 μ mol) was dissolved in TFA (1 mL). After stirring at room temperature for 5–10 min, excess TFA was removed under reduced pressure. The residue was dissolved in

2 mL of water. The product was isolated by semiprep HPLC (Method 1). The fractions at 12.5 min were collected and combined. Lyophilization of the combined fractions afforded the expected product K-3P-RGD₂ as its TFA salt. The yield was 1.7 mg (~78%). ESI-MS: m/z = 2188.5 for $[M + H]^+$ (M = 2187.18 calcd. for $[C_{98}H_{162}N_{24}O_{32}]$).

Lys(HYNIC)₂-PEG₄-E[PEG₄-c(RGDfk)]₂ (K(HYNIC)₂-3P-RGD₂). HYNIC-OSu (4.6 mg, 10 μ mol) and K-3P-RGD₂ (2.2 mg, 1.0 μ mol) were dissolved in DMF (1 mL). After addition of excess DIEA (50 μ mol), the mixture was stirred at room temperature for 7 days. Upon addition of 2 mL water, the pH was adjusted to 4–4.5 using TFA. The product was separated from the mixture using the same HPLC method for K(HYNIC)₂-RGD₂. The fractions at 20.8 min were collected. Lyophilization of the collected fractions afforded K(HYNIC)₂-3P-RGD₂. The yield was 1.2 mg (~43%). ESI-MS: m/z = 2794.9 for $[M + H]^+$ and 1398.0 for $[M + H]^{2+}$ (M = 2793.24 calcd. for $[C_{124}H_{180}N_{30}O_{40}S_2]$).

^{99m}Tc-Labeling. To a clean 5 cc vial were added the K(HYNIC)₂-peptide conjugate solution (25 μ g in 25 μ L water), 0.4 mL of 0.25 M succinate buffer (pH = 4.8), and 0.4 mL of tricine solution (20–40 mg/mL in 0.25 M succinate buffer). After addition of 0.5 mL of ^{99m}TcO₄[−] (740–1110 MBq in saline) and 25 μ L of SnCl₂ (1.0 mg/mL in 0.1 N HCl), the vial was heated at 100 °C for 20–30 min in a boiling water bath. The vial was then allowed to stand at room temperature for ~5 min. A sample of the resulting solution was analyzed by radio-HPLC (Method 2).

Dose Preparation. For biodistribution studies, ^{99m}Tc radiotracers were purified by HPLC. Volatiles in the mobile phase were removed completely under vacuum (<10 mmHg). Doses were prepared by dissolving the residual in saline to ~1 MBq/mL. For imaging studies, doses were prepared by dissolving the radiotracer in saline to ~370 MBq/mL. In the blocking experiment, RGD₂ was dissolved in the dose solution to a concentration of 3.5 mg/mL. The resulting solution was filtered with a 0.20 μ m Millex-LG filter before being injected into animals. Each animal was injected with ~0.1 mL of the dose solution.

In Vitro Whole-Cell Integrin $\alpha_v\beta_3$ Binding Assay. The integrin binding affinity of cyclic RGD peptides was assessed via a cellular competitive displacement assay using ¹²⁵I-echistatin (Perkin-Elmer, Branford, CT) as the radioligand.³³ U87MG cell line was obtained from ATCC (American Type Culture Collection, Manassas, VA). Briefly, U87MG cells were grown in Eagle's Minimum Essential Medium (EMEM) supplemented with 10% fetal bovine serum (FBS, ATCC), 100 IU/mL penicillin, and 100 μ g/mL streptomycin (Invitrogen Co, Carlsbad, CA), at 37 °C in humidified atmosphere containing 5% CO₂. Filter multiscreen DV plates (Millipore, Billerica, MA) were seeded with 1×10^5 glioma cells in binding buffer (20 mM Tris, 150 mM NaCl, 2 mM CaCl₂, 1 mM MnCl₂, 1 mM MgCl₂, 0.1% (wt/vol) bovine serum albumin; and pH 7.4), and ¹²⁵I-echistatin (0.7–1.0 kBq) in the presence of increasing amounts of RGD peptide, incubated for 2 h at room temperature. After removing the unbound ¹²⁵I-echistatin, and being washed 3 \times with binding buffer, hydrophilic PVDF filters were collected. The radioactivity was determined using a Perkin-Elmer Wizard 1480 γ -counter (Shelton, CT). All experiments were carried out twice in triplicate. IC₅₀ values were calculated by fitting the experimental data with the nonlinear regression using GraphPad Prism (GraphPad Software, Inc., San Diego, CA), and reported as an average of

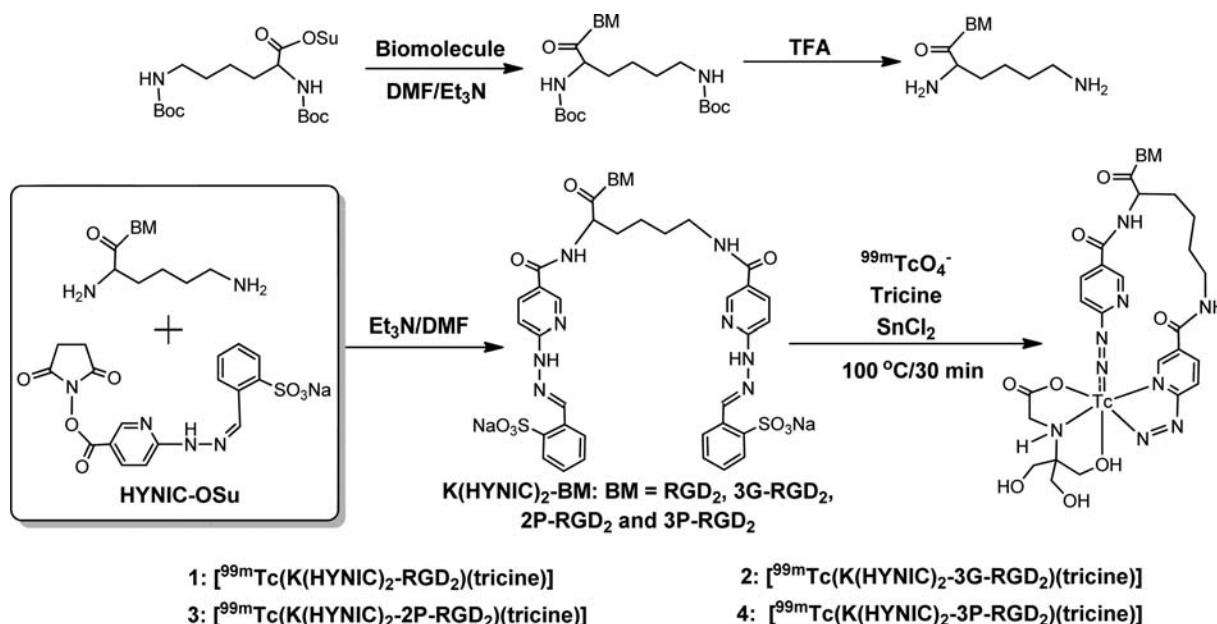
six samples plus/minus the standard deviation. Comparison between two cyclic RGD peptides was made using the one-way ANOVA test. The level of significance was set at $p < 0.05$.

Animal Model. Biodistribution and SPECT/CT imaging studies were performed in compliance with the NIH animal experimentation guidelines (*Principles of Laboratory Animal Care*, NIH Publication No. 86–23, revised 1985). The protocol was approved by the Purdue University Animal Care and Use Committee (PACUC). Female athymic *nu/nu* mice were purchased from Harlan (Indianapolis, IN) at 4–5 weeks of age, and were implanted with 5×10^6 U87MG cells in the shoulder flank. All procedures were performed in a laminar flow cabinet using aseptic techniques. Four weeks after inoculation, the tumor size was 0.1–0.5 g, and animals were used for biodistribution and imaging studies.

Biodistribution. The tumor-bearing athymic nude mice (20–25 g) were randomly selected. Each animal was administered with ~0.1 MBq of the ^{99m}Tc radiotracer by the tail-vein injection. The animals ($n = 4–6$) were sacrificed by sodium pentobarbital overdose (~200 mg/kg) at 60 min postinjection (p.i.). Blood was withdrawn from the heart. Tumors and normal organs (brain, eyes, heart, intestine, kidneys, liver, lungs, muscle, and spleen) were harvested immediately after death, washed with saline, dried with absorbent paper, weighed, and counted to determine the radioactivity accumulation using a Perkin-Elmer Wizard 1480 γ -counter (Shelton, CT). The organ uptake was calculated as the percentage of injected dose per gram of organ mass (%ID/g). Biodistribution data and tumor-to-background (T/B) ratios are reported as an average plus/minus the standard deviation from 4–6 tumor-bearing mice. Comparison of different radiotracers was made using one-way ANOVA followed by pairwise Tukey's posthoc test. The level of significance was set at $p < 0.05$.

SPECT/CT Imaging. SPECT/CT images were obtained using a u-SPECT-II/CT scanner (Milabs, Utrecht, The Netherlands) equipped with a 0.6 mm multipinhole collimator. The glioma-bearing mouse was injected with ~37 MBq of 4 in 0.1 mL saline via the tail vein. At 60 min p.i., the animal was placed into a shielded chamber connected to an isoflurane anesthesia unit (Univentor, Zejtun, Malta). Anesthesia was induced using an air flow rate of 350 mL/min and ~3.0% isoflurane. After induction of anesthesia, the animal was placed supine on the scanning bed. The air flow rate was then reduced to ~250 mL/min with ~2.0% isoflurane. Rectangular scan in regions of the interest (ROIs) from both SPECT and CT was selected on the basis of orthogonal optical images provided by the integrated webcams. After SPECT acquisition (75 projections over 30 min per frame, 2 frames), the animal was then translated into the attached CT scanner and imaged using the "normal" acquisition settings (2 degree intervals) at 45 kV and 500 μ A. After CT acquisition, the animal was allowed to recover in a lead-shielded cage. SPECT reconstruction, data processing, and quantification of organ uptake were performed according to the methods described in our previous reports.^{43,44} The reconstructed images were visualized as both orthogonal slices and maximum intensity projections.

Metabolism. Normal athymic nude mice ($n = 3$) were used for metabolism study. Each animal was administered with ~100 μ Ci of 4 via tail vein. Urine samples were collected at 30 and 120 min p.i. by manual void, and were mixed with equal volume of 50% acetonitrile aqueous solution. The mixture was centrifuged at 8000 rpm. The supernatant was collected and

Chart 1. Synthetic Scheme for Preparation of (HYNIC)₂K-Conjugated Cyclic RGD Peptide Dimers and Their Macrocytic ^{99m}Tc Complexes


filtered with the 0.20 μ m syringe-driven Millex-LG filter unit to remove foreign particles. The filtrate was analyzed by radio-HPLC. Feces samples were collected at 120 min p.i. and suspended in 25% acetonitrile aqueous solution. The resulting mixture was vortexed for ~5 min. After centrifuging at 8000 rpm, the supernatant was collected and filtered with the 0.20 μ m syringe-driven Millex-LG filter unit to remove foreign particles. The filtrate was analyzed by radio-HPLC.

RESULTS

HYNIC-Conjugate Synthesis. Chart 1 shows the synthetic scheme for K(HYNIC)₂-conjugated cyclic RGD peptide dimers. First, the peptide reacted with K(Boc)₂-OSu in the presence of DIEA afforded K(Boc)₂-BM (BM = RGD₂, 3G-RGD₂, 2P-RGD₂, and 3P-RGD₂). Deprotection of Boc-

 Table 1. Radiochemical Purity (RCP) and HPLC Retention Time for ^{99m}Tc-Radiotracers

radiotracer	RCP (%)	HPLC retention (min)
1	>90	14.5
2	>95	13.8
3	>95	14.8
4	>95	15.2

protecting groups in neat TFA gave the intermediates, K-RGD₂, K-3G-RGD₂, K-2P-RGD₂, and K-3P-RGD₂, respectively, which were then allowed to react with excess HYNIC-OSu in the presence of DIEA to afford the final product: K(HYNIC)₂-RGD₂, K(HYNIC)₂-3G-RGD₂, K(HYNIC)₂-2P-RGD₂, and K(HYNIC)₂-3P-RGD₂, respectively. All new cyclic RGD peptide conjugates were purified by semiprep HPLC (Method 1) and characterized by ESI-MS. The mass spectral data were completely consistent with the proposed composition. Their HPLC purities were >95% before being used for the integrin $\alpha_v\beta_3$ binding assay and ^{99m}Tc-labeling.

Integrin $\alpha_v\beta_3$ Binding Affinity. Figure 2 shows the displacement curves of ¹²⁵I-echistatin bound to U87MG cells in the presence of cyclic RGD peptides. For comparison purpose, c(RGDfK) was also evaluated in the same assay. IC₅₀ values were calculated to be 47 \pm 2, 35 \pm 2, 37 \pm 2, 85 \pm 2, and 422 \pm 15 nM for K(HYNIC)₂-2P-RGD₂, K(HYNIC)₂-3P-RGD₂, K(HYNIC)₂-3G-RGD₂, K(HYNIC)₂-RGD₂, and c(RGDfK), respectively. The integrin $\alpha_v\beta_3$ binding affinity follows the order K(HYNIC)₂-3G-RGD₂ \sim K(HYNIC)₂-2P-RGD₂ \sim K(HYNIC)₂-3P-RGD₂ > K(HYNIC)₂-RGD₂ \gg c(RGDfK) (Figure 2), which was very similar to the trend reported for HYNIC and DOTA-conjugated cyclic RGD peptide dimers in our previous communications.^{33,40}

Radiochemistry. Macrocytic ^{99m}Tc complexes 1–4 were prepared (Chart 1) from the reaction of respective K-(HYNIC)₂-conjugated peptide with ^{99m}TcO₄[−] in the presence of excess tricine and stannous chloride. ^{99m}Tc-labeling was completed by heating the reaction mixture at 100 °C for 20–30

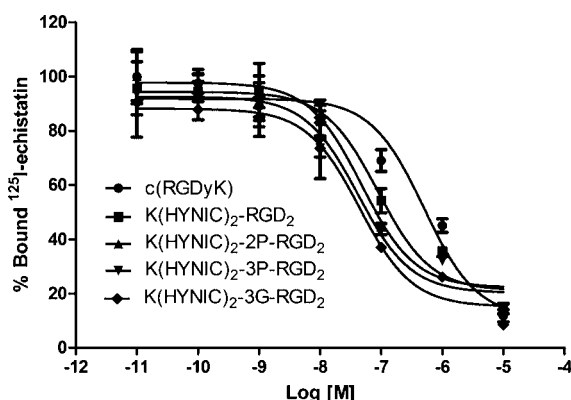


Figure 2. Competitive inhibition curves of ¹²⁵I-echistatin bound to U87MG glioma cells in the presence of increasing concentrations of cyclic RGD peptide. Their IC₅₀ values were calculated to be 47 \pm 2, 35 \pm 2, 37 \pm 2, 85 \pm 1, and 422 \pm 15 nM for K(HYNIC)₂-2P-RGD₂, K(HYNIC)₂-3P-RGD₂, K(HYNIC)₂-3G-RGD₂, K(HYNIC)₂-RGD₂, and c(RGDfK), respectively. The integrin $\alpha_v\beta_3$ binding affinity follows the order: K(HYNIC)₂-3G-RGD₂ \sim K(HYNIC)₂-2P-RGD₂ \sim K(HYNIC)₂-3P-RGD₂ > K(HYNIC)₂-RGD₂ \gg c(RGDfK).

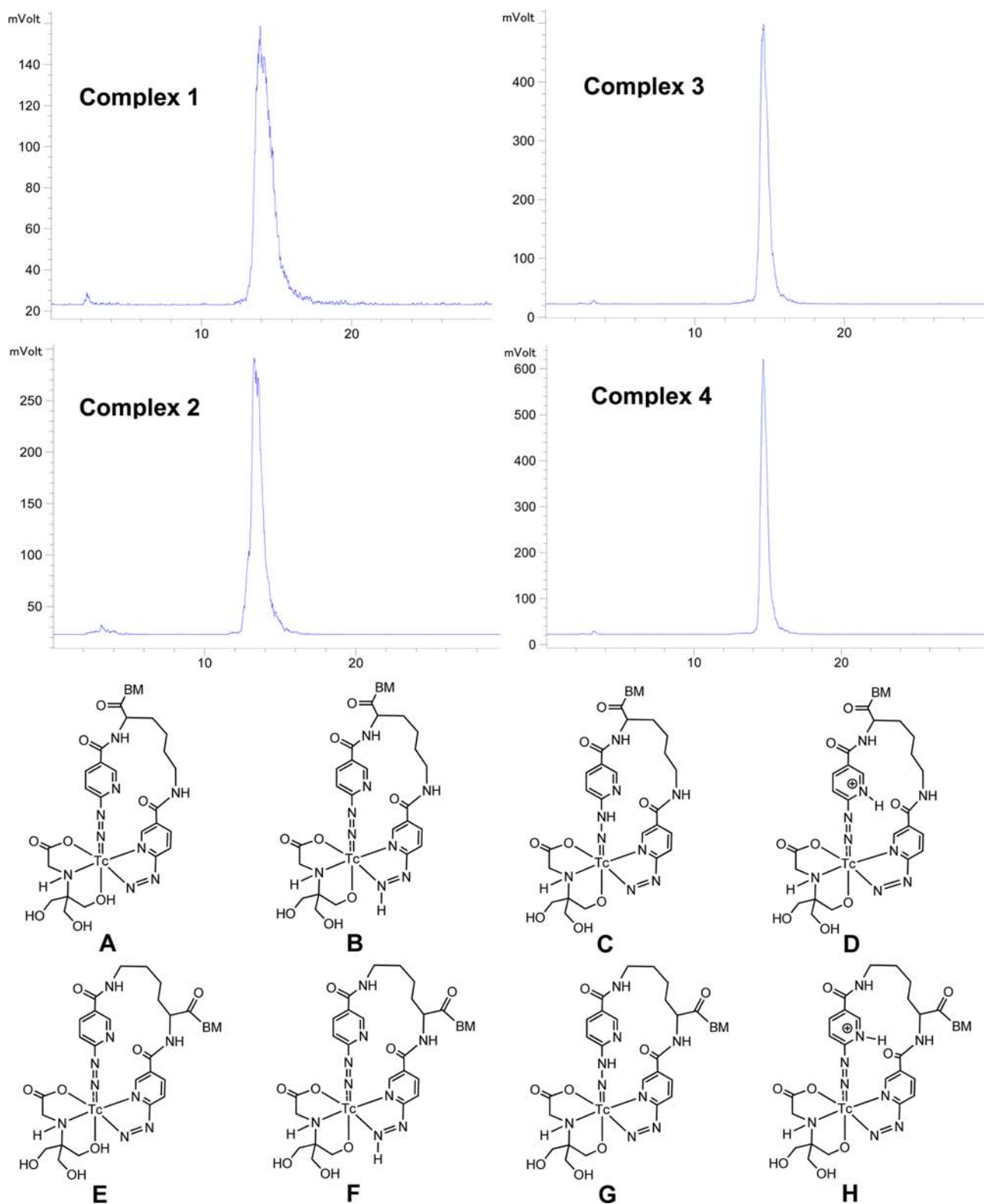


Figure 3. Top: Radio-HPLC chromatograms of **1–4**. Bottom: Structures of possible isomers (**A–H**) in macrocyclic ^{99m}Tc complexes $[\text{}^{99m}\text{Tc}(\text{tricine})(\text{HYNIC})_2\text{K-BM}]$ (BM = RGD₂, 3G-RGD₂, 2P-RGD₂, and 3P-RGD₂).

min. Complexes **1–4** had high radiochemical purity (Table 1: RCP >95%) and high specific activity (~150 GBq/μmol) without chromatographic purification. They also had high solution stability in the kit matrix at room temperature (Figure SII). Excess tricine (10–50 mg/vial) was required to prevent formation of [^{99m}Tc]colloid. If the tricine concentration was

<10 mg/vial, [^{99m}Tc]colloid formation might become significant. If the tricine concentration was >60 mg/vial, the radiolabeling yield was also low (<90%) for ^{99m}Tc radiotracers. Since tricine has buffering capacity at pH = 4–5, there was no need for extra buffering agent. We tried to replace tricine with *N*-(2-hydroxyethyl)glycine and ethylenediamine-*N,N'*-diacetic

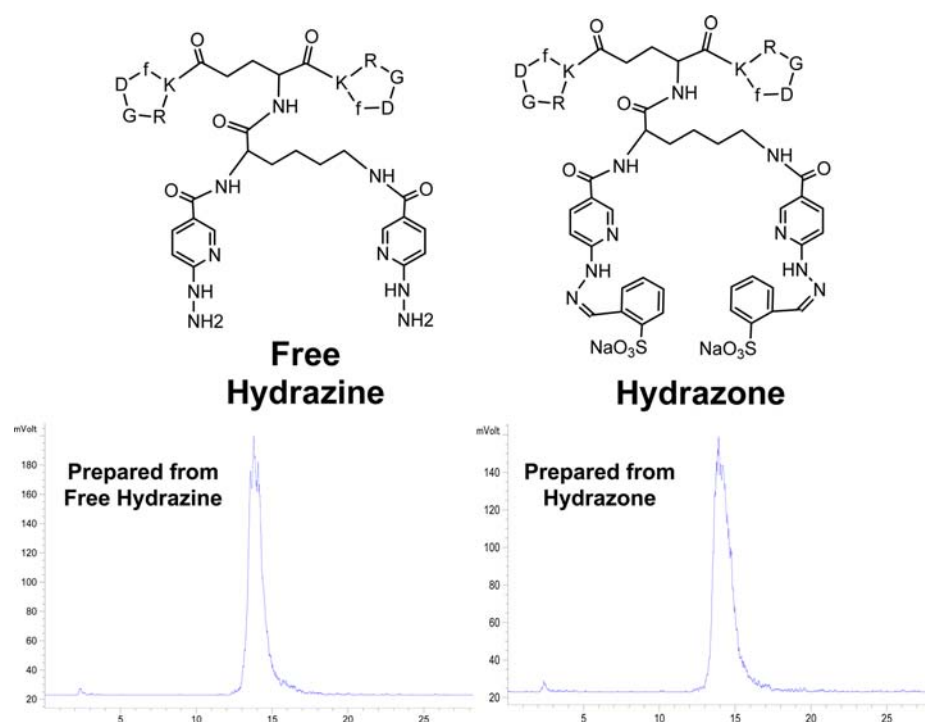


Figure 4. Representative radio-HPLC chromatograms of **1** prepared from free hydrazine (left) and hydrazine (right). The macrocyclic ^{99m}Tc complex prepared from free hydrazine or hydrazine-protected $\text{K}(\text{HYNIC})_2\text{-RGD}_2$ had identical radio-HPLC profiles under the same chromatographic conditions, suggesting that both hydrazone-protecting groups in $\text{K}(\text{HYNIC})_2\text{-RGD}_2$ were removed during ^{99m}Tc chelation.

Table 2. Selected Biodistribution Data of **1–5** in Athymic Nude Mice Bearing U87MG Human Glioma Xenografts at 1 h p.i.

compound	1 ($n = 6$)	2 ($n = 4$)	3 ($n = 4$)	4 ($n = 6$)	5 ($n = 6$)
Blood	0.81 ± 0.04	0.73 ± 0.15	0.99 ± 0.04	0.69 ± 0.16	0.47 ± 0.06
Brain	0.12 ± 0.01	0.13 ± 0.03	0.14 ± 0.03	0.14 ± 0.02	0.17 ± 0.03
Eyes	0.98 ± 0.09	0.92 ± 0.19	1.27 ± 0.18	1.09 ± 0.21	1.40 ± 0.13
Heart	1.02 ± 0.06	1.06 ± 0.22	1.28 ± 0.30	1.12 ± 0.18	1.67 ± 0.15
Intestine	9.29 ± 1.66	6.87 ± 2.98	11.40 ± 0.97	10.30 ± 5.01	9.45 ± 1.31
Kidneys	12.21 ± 0.93	8.49 ± 1.28	9.94 ± 1.65	9.28 ± 1.14	12.28 ± 1.09
Liver	1.55 ± 0.27	2.61 ± 0.59	2.74 ± 0.50	3.05 ± 0.54	2.92 ± 0.77
Lungs	2.70 ± 0.04	3.17 ± 0.50	2.93 ± 0.65	2.68 ± 0.40	4.25 ± 0.63
Muscle	0.92 ± 0.11	0.79 ± 0.15	1.10 ± 0.32	0.85 ± 0.11	1.12 ± 0.15
Spleen	1.57 ± 0.17	1.74 ± 0.98	1.78 ± 0.26	1.92 ± 0.38	3.11 ± 0.18
Tumor	3.78 ± 0.81	7.46 ± 1.68	9.74 ± 1.65	8.59 ± 1.52	7.24 ± 0.95
Tumor/Blood	4.70 ± 1.22	10.88 ± 0.82	9.87 ± 1.65	15.88 ± 2.87	15.36 ± 1.01
Tumor/Liver	2.43 ± 0.21	2.92 ± 0.64	3.66 ± 0.13	2.98 ± 0.18	2.55 ± 0.36
Tumor/Lung	1.40 ± 0.28	2.52 ± 0.18	3.60 ± 0.13	3.30 ± 0.14	1.71 ± 0.05
Tumor/Muscle	4.23 ± 1.27	9.64 ± 0.46	8.68 ± 1.84	10.76 ± 1.92	6.58 ± 1.58

acid, but the RCP for their ^{99m}Tc complexes was low ($<70\%$). Tricine remains the best with respect to RCP of ^{99m}Tc complexes.

Isomerism. Figure 3 shows radio-HPLC chromatograms of **1–4**. Due to the asymmetric nature of $\text{K}(\text{HYNIC})_2$ in bonding to Tc, there are several possible isomers (Figure 3: A–H). Isomers A–D and E–H are indistinguishable in aqueous solution since the proton can be on N or O atom. Both tricine and its Tc chelate are chiral once $[\text{K}(\text{HYNIC})_2\text{-BM}(\text{tricine})]$ is formed. The combination of A–H with chiral centers in $[\text{K}(\text{HYNIC})_2](\text{tricine})$ will result in many isomers. It was not surprising that more than two radiometric peaks (Figure 3: top) were observed in the radio-HPLC chromatograms of **1** and **2**. Attempts to separate these peaks using various chromatographic conditions (different columns,

flow rates, and ionic strength) were unsuccessful. Complexes **3** and **4** always show one single radiometric peak in their radio-HPLC chromatograms, most likely due to the much larger size of the cyclic RGD peptide (>2000 Da) than that of $[\text{K}(\text{HYNIC})_2](\text{tricine})$ (~ 670 Da). It is important to note that one radiometric peak does not necessarily mean only one isomer or one species.

We also prepared $\text{K}(\text{HYNIC})_2\text{-RGD}_2$ as the unprotected free hydrazine (Figure 4: top). The purpose was to determine if the two hydrazone-protecting groups in $\text{K}(\text{HYNIC})_2\text{-RGD}_2$ were removed during ^{99m}Tc -labeling. We found that the same macrocyclic ^{99m}Tc complex was prepared from the free hydrazine or hydrazine-protected $\text{K}(\text{HYNIC})_2\text{-RGD}_2$, as evidenced by their almost identical radio-HPLC profiles (Figure 4: bottom) under identical chromatographic con-

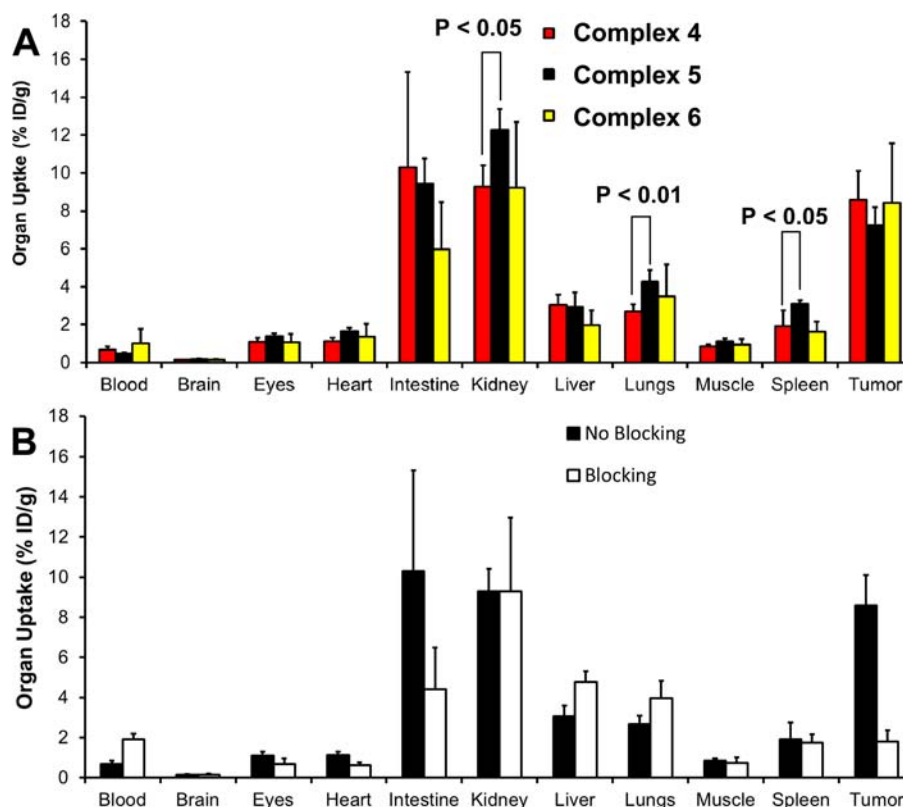


Figure 5. (A) Comparison of 60 min biodistribution data for [$^{99m}\text{Tc}((\text{HYNIC})_2\text{K-3P-RGD}_2)(\text{tricine})$] (4: $n = 6$), [$^{99m}\text{Tc}(\text{HYNIC-3P-RGD}_2)(\text{tricine})$] (5: $n = 6$), and [$^{99m}\text{Tc}((\text{HYNIC})\text{K}(\text{NIC})\text{-3P-RGD}_2)(\text{tricine})$] (6: $n = 4$) in athymic nude mice bearing U87MG glioma xenografts to show the impact of ^{99m}Tc chelate on biodistribution properties of ^{99m}Tc radiotracers. (B) Comparison of the selected 60-min biodistribution data of 4 in athymic nude mice ($n = 6$) bearing U87MG glioma xenografts in the absence/presence of excess $\text{E}[\text{c}(\text{RGDfK})]_2$ (RGD_2 : 350 $\mu\text{g}/\text{mouse}$ or 14 mg/kg) to demonstrate its specificity in binding to integrin $\alpha_v\beta_3$.

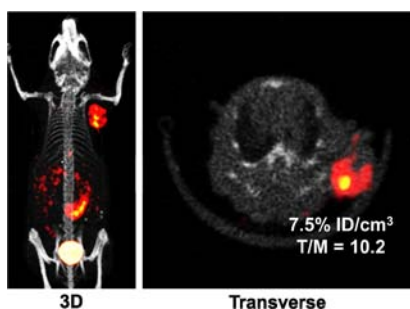


Figure 6. 3D and transverse views of SPECT/CT image of an athymic nude mouse bearing U87 M human glioma xenografts ($\sim 0.2 \text{ cm}^3$). The animal was administered with $\sim 50 \text{ MBq}$ of 4. There was no significant radioactivity accumulation in kidneys, liver, lungs, and muscle. However, there was significant radioactivity accumulation in the intestines, which is consistent with the biodistribution data (Table 2).

ditions. We believe that both hydrazone-protecting groups in $\text{K}(\text{HYNIC})_2$ were removed during ^{99m}Tc chelation. If the hydrazone-protecting groups in $\text{K}(\text{HYNIC})_2\text{-RGD}_2$ were not removed during ^{99m}Tc -labeling, macrocyclic ^{99m}Tc complexes prepared from the hydrazone-protected $\text{K}(\text{HYNIC})_2\text{-RGD}_2$ would have had completely different radio-HPLC profiles (retention times and patterns) from those from the free hydrazine.

Biodistribution. Table 1 lists the selected biodistribution data of 1–5. Complex 5 was evaluated in the same model for comparison purposes. The 60 min data were used since the

blood radioactivity was relatively low. Among the five radiotracers evaluated in this study, 1 had lowest tumor uptake ($3.78 \pm 0.81\% \text{ ID/g}$) and the poorest tumor/background ratios (Table 2). The tumor uptake of 2–5 was comparable within the experimental errors, which was completely consistent with similar integrin $\alpha_v\beta_3$ binding affinity of the corresponding cyclic RGD peptides (Figure 2). The uptake of 2–4 in the kidneys, lungs, and spleen was lower than that of 5 (Table 2). These data suggest that the targeting biomolecule has significant impact on the radiotracer uptake in both tumors and normal organs. Figure 5A compares the 60 min biodistribution data of 4–6. Biodistribution data for 6 were from our previous report.³² It was quite obvious that replacing [$^{99m}\text{Tc}(\text{HYNIC})\text{-}(\text{tricine})$](TPPTS)] with [$^{99m}\text{Tc}(\text{K}(\text{HYNIC})_2)(\text{tricine})$] had little impact on the radiotracer tumor uptake, but it significantly influenced the uptake of ^{99m}Tc radiotracers in the intestines, kidneys, lungs, and spleen. Since $\text{K}(\text{HYNIC})_2$ is structurally similar to $\text{HYNIC-K}(\text{NIC})$, we were not surprised that 4 and 6 shared very similar biodistribution properties in the tumor and normal organs (Figure 5A).

Integrin $\alpha_v\beta_3$ Specificity. Figure 5B compares the organ uptake ($\% \text{ ID/g}$) of 4 in the absence/presence of excess RGD_2 at 60 min p.i. Co-injection of excess RGD_2 significantly blocked its tumor uptake ($1.81 \pm 0.56\% \text{ ID/g}$ with RGD_2 vs $8.59 \pm 1.52\% \text{ ID/g}$ without RGD_2). The uptake of 4 in the intestine was $10.30 \pm 5.01\% \text{ ID/g}$ without RGD_2 and $4.41 \pm 2.07\% \text{ ID/g}$ in the presence of excess RGD_2 . These data suggest that intestine is integrin $\alpha_v\beta_3$ -positive. The blood radioactivity level was higher in animals administered with excess RGD_2 than that

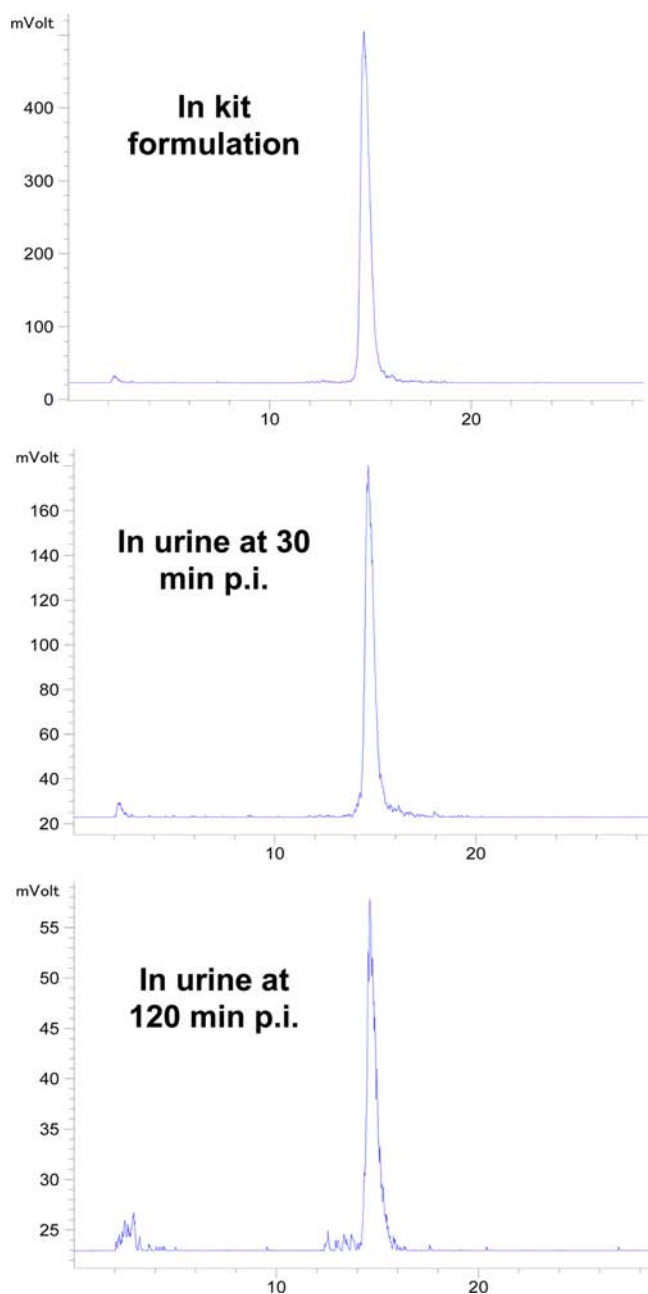


Figure 7. Representative radio-HPLC chromatograms for radiotracer **4** in the saline before injection, and in the urine at 30 and 120 min p.i.

without excess RGD₂, probably due to the reduced uptake in the integrin $\alpha_v\beta_3$ -positive organs. Similar results were reported for other integrin $\alpha_v\beta_3$ -targeted radiotracers.^{32–40}

SPECT/CT Imaging. Figure 6 shows the 3D and transverse views of SPECT/CT image of a glioma-bearing mouse. The tumor ($\sim 0.2 \text{ cm}^3$) was clearly visualized by SPECT/CT with excellent contrast. The tumor uptake was $\sim 7.5\% \text{ID}/\text{cm}^3$ on the basis of SPECT quantification. The tumor/muscle ratio was $>10:1$. The uptake of **4** in the kidneys, liver, lungs, and muscle was relatively low. Its high intestine uptake was supported by the biodistribution data (Table 2). The SPECT/CT data clearly showed that **4** is an excellent radiotracer for noninvasive imaging of U87MG gliomas with high integrin $\alpha_v\beta_3$ expression on both tumor cells and the tumor neovasculature.^{32,39}

Metabolism. We examined the metabolic stability of **4** using normal mice ($n = 3$). The radioactivity recovery from the urine and feces samples was $>95\%$. Figure 7 shows radio-HPLC chromatograms of **4** in saline before injection (top) and in urine at 30 min p.i. (middle) and 120 min p.i. (bottom). There was very little metabolism in the urine samples at 30 and 120 min p.i. Attempts were made to isolate sufficient radioactivity from feces for HPLC, but they were unsuccessful because $>90\%$ of collected radioactivity was found in the urine. We believe that **4** had a high metabolic stability during its excretion in athymic nude mice. Its metabolic stability was similar to that reported for **6**,³² most likely due to their structural similarity (Figure 1: B and C).

DISCUSSION

In this study, we evaluated K(HYNIC)₂ as a BFC for $^{99\text{m}}\text{Tc}$ -labeling of cyclic RGD peptides and compared three chelating systems (Figure 1: A–C) with respect to the biodistribution of their $^{99\text{m}}\text{Tc}$ radiotracers. We found that K(HYNIC)₂-conjugated RGD peptides had integrin $\alpha_v\beta_3$ binding affinity comparable to that of their HYNIC analogs.^{34,35} A major advantage of K(HYNIC)₂ over the ternary ligand system (HYNIC, tricine, and TPPTS) is the use of SnCl₂ as a reducing agent. This is very important for $^{99\text{m}}\text{Tc}$ -labeling of small biomolecules with one or more disulfide linkages, which are vital to maintaining their structural rigidity and receptor binding affinity. The use of TPPTS at elevated temperatures may destroy the S–S disulfide bonds. The disadvantage of K(HYNIC)₂ is that [$^{99\text{m}}\text{Tc}(\text{K}(\text{HYNIC})_2)(\text{tricine})$] has more than 2 isomers, which were not separable under chromatographic conditions used in this study. Similar results were also obtained for macrocyclic complexes [$^{99\text{m}}\text{Tc}(\text{HYNIC}-\text{K}(\text{NIC})-\text{BM})(\text{tricine})$].³¹ Future research will be directed toward developing symmetrical bis-HYNIC analogs that form macrocyclic $^{99\text{m}}\text{Tc}$ chelates with two or fewer isomers.

[$^{99\text{m}}\text{Tc}(\text{K}(\text{HYNIC})_2)(\text{tricine})$] (molecular weight: $\sim 670 \text{ Da}$) has an overall neutral charge, and is smaller than [$^{99\text{m}}\text{Tc}(\text{HYNIC})(\text{tricine})(\text{TPPTS})$] (molecular weight: $\sim 970 \text{ Da}$). However, replacing [$^{99\text{m}}\text{Tc}(\text{HYNIC})(\text{tricine})(\text{TPPTS})$] with [$^{99\text{m}}\text{Tc}(\text{K}(\text{HYNIC})_2)(\text{tricine})$] had little impact on the tumor uptake of $^{99\text{m}}\text{Tc}$ radiotracers (Figure 5A), suggesting that changing $^{99\text{m}}\text{Tc}$ chelates had no adverse effect on their integrin $\alpha_v\beta_3$ binding affinity. We also found that **4** had significantly less uptake than **5** in kidneys, lungs, and spleen (Figure 5A: $p < 0.05$), strongly suggesting that $^{99\text{m}}\text{Tc}$ chelates had significant impact on biodistribution of their $^{99\text{m}}\text{Tc}$ radiotracers. The metabolic stability of **4** was similar to that of **5** and **6**.^{32,33} Our previous studies showed that the metabolic instability of **6** during hepatobiliary excretion had little impact on its %ID/g tumor uptake and the linear relationship between the tumor uptake of **6** and integrin $\alpha_v\beta_3$ expression levels.³³

Since the same macrocyclic $^{99\text{m}}\text{Tc}$ complex was prepared from K(HYNIC)₂-RGD₂ in its unprotected and hydrazone-protected forms, we believe that the two hydrazone-protecting groups in K(HYNIC)₂ were removed during $^{99\text{m}}\text{Tc}$ -labeling. Thus, [$^{99\text{m}}\text{Tc}(\text{K}(\text{HYNIC})_2)(\text{tricine})$] (Figure 1C) has a structure similar to that of [$^{99\text{m}}\text{Tc}(\text{HYNIC}-\text{K}(\text{NIC}))(\text{tricine})$] (Figure 1B), the composition of which was confirmed by LC-MS data.³¹ However, it remains unclear about the exact structure of [$^{99\text{m}}\text{Tc}(\text{K}(\text{HYNIC})_2)(\text{tricine})$]. It is quite possible that one HYNIC is monodentate and the other is bidentate in [$^{99\text{m}}\text{Tc}(\text{K}(\text{HYNIC})_2)(\text{tricine})$] (Figure 1C). Anionic monodentate pyridyldiazenido (Figure 3: A and E), neutral bidentate

pyridyldiazene (Figure 3: B and F), anionic bidentate pyridyldiazene (Figure 3: C and G), and monodentate pyridiniumdiazene (Figure 3: D and H) have been found in many Tc(III) and Re(III) complexes,^{45–51} such as $[\text{TcCl}_3(\text{HN}=\text{NC}_5\text{H}_4\text{N})(\text{N}=\text{NC}_5\text{H}_4\text{NH})]$ and $[\text{ReCl}_2(\text{PPh}_3)(\text{N}=\text{NC}_5\text{H}_4\text{N})(\text{HN}=\text{NC}_5\text{H}_4\text{N})]$, both of which were characterized by X-ray crystallography.^{46,47} Because of bidentate HYNIC, the backbone rotations in $[\text{99mTc}(\text{K}(\text{HYNIC})_2)(\text{tricine})]$ will be limited, preventing interconversion of conformational isomers. It is not surprising that >2 radiometric peaks were observed in HPLC chromatograms of **1** and **2** (Figure 3: A and B). However, in the absence of solid-state structure and NMR studies, this explanation remains largely a speculation. Structure studies of macrocyclic $^{99\text{m}}\text{Tc}$ complexes will help us understand the coordination chemistry of bis-HYNIC chelators in their macrocyclic $^{99\text{m}}\text{Tc}$ complexes.

CONCLUSION

This study shows that $\text{K}(\text{HYNIC})_2$ is useful as a BFC for $^{99\text{m}}\text{Tc}$ -labeling of small biomolecules, such as cyclic RGD peptides. Replacing $[\text{99mTc}(\text{HYNIC})(\text{tricine})(\text{TPPTS})]$ with $[\text{99mTc}(\text{K}(\text{HYNIC})_2)(\text{tricine})]$ had little impact on the tumor uptake of radiotracers; but it significantly affected the radiotracer uptake in kidneys, lungs, and spleen. Since $[\text{99mTc}(\text{K}(\text{HYNIC})_2)(\text{tricine})]$ exists in solution as several isomers, future research should be directed toward developing symmetrical bis-HYNIC analogs that form macrocyclic $^{99\text{m}}\text{Tc}$ complexes with two or fewer isomers.

ASSOCIATED CONTENT

Supporting Information

Radio-HPLC chromatograms of **4** (Figure SI1) at 1 and 24 h postlabeling to show its solution stability at room temperature. This material is available free of charge via the Internet at <http://pubs.acs.org>.

AUTHOR INFORMATION

Corresponding Author

*Phone: 765-494-0236. Fax 765-496-1377. E-mail: liu100@purdue.edu

Notes

The authors declare no competing financial interest.

ACKNOWLEDGMENTS

This work was supported by Purdue University, the Indiana Clinical and Translational Sciences Institute funded, in part, by grant Number TR000006 (Clinical and Translational Award) from the National Institutes of Health, National Center for advancing Translational Science, R01 CA115883 (S.L.) from the National Cancer Institute, and KG111333 (Y.Z. and S.L.) from the Susan G. Komen Breast Cancer Foundation.

REFERENCES

- (1) Abrams, M. J.; Juweid, M.; tenKate, C. I.; Schwartz, D. A.; Hauser, M. M.; Gaul, F. E.; Fuccello, A. J.; Rubin, R. H.; Strauss, H. W.; and Fischman, A. J. (1990) Technetium-99m-human polyclonal IgG radiolabeled via the hydrazine nicotinamide derivative for imaging focal sites of infection in rats. *J. Nucl. Med.* 31, 2022–2028.
- (2) Schwartz, D. A.; Abrams, M. J.; Hauser, M. M.; Gaul, F. E.; Larsen, S. K.; Rauh, D.; and Zubietta, J. (1991) Preparation of hydrazine-modified proteins and their use for the synthesis of $^{99\text{m}}\text{Tc}$ -protein conjugates. *Bioconjugate Chem.* 2, 333–336.
- (3) Ultee, M. E.; Bridger, G. J.; Abrams, M. J.; Longley, C. B.; Burton, C. A.; Larsen, S.; Henson, G. W.; Padmanabhan, S.; Gaul, F. E.; and Schwartz, D. A. (1997) Tumor imaging with technetium-99m-labeled hydrazinonicotinamide-Fab' conjugates. *J. Nucl. Med.* 38, 133–138.
- (4) Bridger, G. J.; Abrams, M. J.; Padmanabhan, S.; Gaul, F. E.; Larsen, S.; Henson, G. W.; Schwartz, D. A.; Burton, C. A.; and Ultee, M. E. (1996) A comparison of cleavable and noncleavable hydrazinopyridine linkers for the $^{99\text{m}}\text{Tc}$ -labeling of Fab' monoclonal antibody fragment. *Bioconjugate Chem.* 7, 255–264.
- (5) Babich, J. W.; Solomon, H.; Pike, M. C.; Kroon, D.; Graham, W.; Abrams, M. J.; Tompkins, R. G.; Rubin, R. H.; and Fischman, A. J. (1993) Technetium-99m labeled hydrazine nicotinamide derivatized chemotactic peptide analogs for imaging focal sites of bacterial infection. *J. Nucl. Med.* 34, 1967–1974.
- (6) Babich, J. W., and Fischman, A. J. (1995) Effect of "co-ligand" on the biodistribution of $^{99\text{m}}\text{Tc}$ -labeled hydrazine nicotinic acid derivatized chemotactic peptides. *Nucl. Med. Biol.* 22, 25–30.
- (7) Babich, J. W.; Graham, W.; Barrow, S. A.; and Fischman, A. J. (1995) Comparison of the infection imaging properties of a $^{99\text{m}}\text{Tc}$ -labeled chemotactic peptide with ^{111}In IgG. *Nucl. Med. Biol.* 22, 643–648.
- (8) Decristoforo, C., and Mather, S. J. (1999) $^{99\text{m}}\text{Tc}$ -labeled peptide-HYNIC conjugates: effect of lipophilicity and stability on biodistribution. *Nucl. Med. Biol.* 26, 389–396.
- (9) Decristoforo, C., and Mather, S. J. (1999) Preparation, $^{99\text{m}}\text{Tc}$ -labeling, and in vitro characterization of HYNIC and N_3S modified RC-160 and $[\text{Tyr}^3]\text{Octreotide}$. *Bioconjugate Chem.* 10, 431–438.
- (10) Decristoforo, C., and Mather, S. J. (1999) Technetium-99m somatostatin analogues: effect of labeling methods and peptide sequence. *Eur. J. Nucl. Med.* 26, 869–876.
- (11) Decristoforo, C.; Melendez, L.; Sosabowski, J. K.; and Mather, S. J. (2000) $^{99\text{m}}\text{Tc}$ -HYNIC- $[\text{Tyr}^3]$ -octreotide for imaging somatostatin-receptor-positive tumors: preclinical evaluation and comparison with ^{111}In -Octreotide. *J. Nucl. Med.* 41, 1114–1119.
- (12) Bangard, M.; Béhé, M.; Guhlke, S.; Otte, R.; Bender, H.; Maecke, H. R.; and Birsack, H. J. (2000) Detection of somatostatin receptor-positive tumours using the new $^{99\text{m}}\text{Tc}$ -tricine-HYNIC-D-Phe¹-Tyr³-octreotide: first results in patients and comparison with ^{111}In -DTPA-D-Phe¹-Tyr³-octreotide. *Eur. J. Nucl. Med.* 27, 628–637.
- (13) Decristoforo, C.; Mather, S. J.; Cholewinski, W.; Donnemiller, E.; Riccabona, G.; and Moncayo, R. (2000) $^{99\text{m}}\text{Tc}$ -EDDA/HYNIC-TOC: a new $^{99\text{m}}\text{Tc}$ -labeled radiopharmaceutical for imaging somatostatin receptor-positive tumors: first clinical results and intra-patient comparison with ^{111}In -labeled octreotide derivatives. *Eur. J. Nucl. Med.* 27, 1318–1325.
- (14) Laverman, P.; Dams, E.; Th, M.; Oyen, W. J. G.; Storm, G.; Koenders, E. B.; Prevost, R.; van der Meer, J. W. M.; Corstens, F. H. M.; and Boerman, O. C. (1999) A novel method to label liposomes with $^{99\text{m}}\text{Tc}$ by the hydrazine nicotinyl derivative. *J. Nucl. Med.* 40, 192–197.
- (15) Zhang, Y. M.; Liu, N.; Zhu, Z. H.; Ruszkowski, M.; and Hnatowich, D. J. (2000) Influence of different chelators (HYNIC, MAG_3 and DTPA) on tumor cell accumulation and mouse biodistribution of technetium-99m labeled antisense DNA. *Eur. J. Nucl. Med.* 27, 1700–1707.
- (16) Hnatowich, D. J.; Winnard, P., Jr.; Virzi, F.; Santo, T.; Smith, C. L.; Cantor, C. R.; and Ruszkowski, M. (1995) Technetium-99m labeling of DNA oligonucleotides. *J. Nucl. Med.* 36, 2306–2314.
- (17) Guo, W.; Hinkle, G. H.; and Lee, R. J. (1999) $^{99\text{m}}\text{Tc}$ -HYNIC-folate: a novel receptor-based targeted radiopharmaceutical for tumor imaging. *J. Nucl. Med.* 40, 1563–1569.
- (18) Ono, M.; Arano, Y.; Mukai, T.; Uehara, T.; Fujioka, Y.; Ogawa, K.; Namba, S.; Nakayama, M.; Saga, T.; Konishi, J.; Horiuchi, K.; Yokoyama, A.; and Saji, H. (2001) Plasma protein binding of $^{99\text{m}}\text{Tc}$ -labeled hydrazine nicotinamide derivatized polypeptides and peptides. *Nucl. Med. Biol.* 28, 155–164.
- (19) Edwards, D. S.; Liu, S.; Ziegler, M. C.; Harris, A. R.; Crocker, A. C.; Heminway, S. J.; Barrett, J. A.; Bridger, G. J.; Abrams, M. J.; and Higgins, J. D. (1999) RP463: A stabilized technetium-99m complex of

a hydrazinonicotinamide conjugated chemotactic peptide for infection imaging. *Bioconjugate Chem.* 10, 884–891.

(20) Brouwers, A. H., Laverman, P., Boerman, O. C., Oyen, W. J. G., Barrett, J. A., Harris, T. D., Edwards, D. S., and Corstens, F. H. M. (2000) A ^{99m}Tc -labeled leukotriene B4 receptor antagonist for scintigraphic detection of infection in rabbits. *Nucl. Med. Commun.* 21, 1043–1050.

(21) Edwards, D. S., Liu, S., Barrett, J. A., Harris, A. R., Looby, R. J., Ziegler, M. C., Heminway, S. J., and Carroll, T. R. (1997) A new and versatile ternary ligand system for technetium radiopharmaceuticals: water soluble phosphines and tricine as coligands in labeling a hydrazino nicotinamide-modified cyclic glycoprotein IIb/IIIa receptor antagonist with ^{99m}Tc . *Bioconjugate Chem.* 8, 146–154.

(22) Liu, S., Edwards, D. S., Ziegler, M. C., Harris, A. R., Hemingway, S. J., and Barrett, J. A. (2001) ^{99m}Tc -Labeling of a hydrazinonicotinamide-conjugated vitronectin receptor antagonist. *Bioconjugate Chem.* 12, 624–629.

(23) Liu, S., Hsieh, W. Y., Kim, Y. S., and Mohammed, S. I. (2005) Effect of coligands on biodistribution characteristics of ternary ligand ^{99m}Tc complexes of a HYNIC-conjugated cyclic RGDfK dimer. *Bioconjugate Chem.* 16, 1580–1588.

(24) Liu, S., Hsieh, W. Y., Jiang, Y., Kim, Y. S., Sreerama, S. G., Chen, X., Jia, B., and Wang, F. (2007) Evaluation of a ^{99m}Tc -labeled cyclic RGD tetramer for noninvasive imaging integrin $\alpha_v\beta_3$ -positive breast cancer. *Bioconjugate Chem.* 18, 438–446.

(25) Liu, S., Kim, Y. S., Hsieh, W. Y., and Sreerama, S. G. (2008) Coligand effects on solution stability, biodistribution and metabolism of ^{99m}Tc -labeled cyclic RGDfK tetramer. *Nucl. Med. Biol.* 35, 111–121.

(26) Liu, S., Edwards, D. S., Harris, A. R., Heminway, S. J., and Barrett, J. A. (1999) Technetium complexes of a hydrazinonicotinamide-conjugated cyclic peptide and 2-hydrazinopyridine: Synthesis and characterization. *Inorg. Chem.* 38, 1326–1335.

(27) Liu, S., Ziegler, M. C., and Edwards, D. S. (2000) Radio-LC-MS for the characterization of ^{99m}Tc -labeled bioconjugates. *Bioconjugate Chem.* 11, 113–117.

(28) Liu, S., and Edwards, D. S. (1999) ^{99m}Tc -labeled small peptides as diagnostic radiopharmaceuticals. *Chem. Rev.* 99, 2235–2268.

(29) Liu, S. (2005) 6-Hydrazinonicotinamide derivatives as bifunctional coupling agents for ^{99m}Tc -labeling of small biomolecules. *Top. Curr. Chem.* 252, 117–153.

(30) Meszaros, L. K., Dose, A., Biagini, S. C. G., and Blower, P. J. (2010) Hydrazinonicotinic acid (HYNIC) – coordination chemistry and applications in radiopharmaceutical chemistry. *Inorg. Chim. Acta* 363, 1059–1069.

(31) Purohit, A., Liu, S., Casebier, D., Haber, S. B., and Edwards, D. S. (2004) Pyridine-containing HYNIC-derivatives as potential bifunctional chelators for ^{99m}Tc -labeling of small biomolecules. *Bioconjugate Chem.* 15, 728–737.

(32) Zhou, Y., Kim, Y. S., Lu, X., and Liu, S. (2012) Evaluation of ^{99m}Tc -labeled cyclic RGD dimers: impact of cyclic RGD peptides and ^{99m}Tc chelates on biological properties. *Bioconjugate Chem.* 23, 586–595.

(33) Wang, L., Kim, Y. S., Shi, J., Zhai, S., Jia, B., Liu, Z., Zhao, H., Wang, F., Chen, X., and Liu, S. (2009) Improving tumor targeting capability and pharmacokinetics of ^{99m}Tc -labeled cyclic RGD dimers with PEG₄ linkers. *Mol. Pharmaceutics* 6, 231–245.

(34) Shi, J., Wang, L., Kim, Y. S., Zhai, S., Liu, Z., Chen, X., and Liu, S. (2008) Improving tumor uptake and excretion kinetics of ^{99m}Tc -labeled cyclic Arginine-Glycine-Aspartic (RGD) dimers with triglycine linkers. *J. Med. Chem.* 51, 7980–7990.

(35) Shi, J., Wang, L., Kim, Y. S., Jia, B., Zhao, H., Wang, F., and Liu, S. (2009) $^{99m}\text{TcO}(\text{MAG}_2\text{-}3\text{G}_3\text{-dimer})$: A new integrin $\alpha_v\beta_3$ -targeted radiotracer with high tumor uptake and favorable pharmacokinetics. *Eur. J. Nucl. Med. Mol. Imaging* 36, 1874–1884.

(36) Shi, J., Wang, L., Kim, Y. S., Zhai, S., Liu, Z., Chen, X., and Liu, S. (2009) Improving tumor uptake and pharmacokinetics of ^{64}Cu -labeled cyclic RGD dimers with Gly₃ and PEG₄ linkers. *Bioconjugate Chem.* 20, 750–759.

(37) Shi, J., Wang, L., Kim, Y. S., Chakraborty, S., Jia, B., Wang, F., and Liu, S. (2009) 2-Mercaptoacetyl-glycyl-glycyl (MAG₂) as a bifunctional chelator for ^{99m}Tc -labeling of cyclic RGD dimers: effects of technetium chelate on tumor uptake and pharmacokinetic. *Bioconjugate Chem.* 20, 1559–1568.

(38) Chakraborty, S., Liu, S., Kim, Y. S., Shi, J., Zhou, Y., and Wang, F. (2011) Evaluation of ^{111}In -labeled cyclic RGD peptides: tetrameric not tetravalent. *Bioconjugate Chem.* 21, 969–978.

(39) Zhou, Y., Kim, Y. S., Chakraborty, S., Shi, J., Gao, H., and Liu, S. (2011) ^{99m}Tc -Labeled cyclic RGD peptides for noninvasive monitoring of tumor integrin $\alpha_v\beta_3$ expression. *Mol. Imaging* 10, 386–397.

(40) Shi, J., Zhou, Y., Chakraborty, S., Kim, Y. S., Jia, B., Wang, F., and Liu, S. (2011) Evaluation of ^{111}In -labeled cyclic RGD peptides: effects of peptide and PEG₄ multiplicity on their tumor uptake, excretion kinetics and metabolic stability. *Theranostics* 1, 322–340.

(41) Shi, J., Jia, B., Kim, Y. S., Chakraborty, S., Zhou, Y., Wang, F., and Liu, S. (2011) Impact of bifunctional chelators on biological properties of ^{111}In -labeled cyclic peptide RGD dimers. *Amino Acids* 41, 1059–1070.

(42) Harris, T. D., Sworin, M., Williams, N., Rajopadhye, M., Dampousse, P. R., Glowacka, D., Poirier, M. J., and Yu, K. (1998) Synthesis of stable hydrazones of a hydrazinonicotinyl-modified peptide for the preparation of ^{99m}Tc -labeled radiopharmaceuticals. *Bioconjugate Chem.* 10, 808–814.

(43) Shao, G., Zhou, Y., and Liu, S. Monitoring glioma growth and tumor necrosis with u-SPECT-II/CT for by targeting integrin $\alpha_v\beta_3$. *Mol. Imaging* in press.

(44) Zhou, Y., Shao, G., Wang, F., and Liu, S. (2012) Imaging breast cancer lung metastasis by u-SPECT-II/CT with an integrin $\alpha_v\beta_3$ -targeted radiotracer ^{99m}Tc -3P-RGD₂. *Theranostics* 2, 577–587.

(45) Babich, J. W., Coco, W. G., Barrow, S. A., Fischman, A. J., Femia, F. J., and Zubieta, J. (2000) ^{99m}Tc -labeled chemotactic peptides: influence of coligands on distribution of molecular species and infection imaging properties. Synthesis and structural characterization of model complexes with the $\{\text{Re}(\eta^2\text{-HNNC}_5\text{H}_4\text{N})(\eta^1\text{-HNNC}_5\text{H}_4\text{N})\}$ core. *Inorg. Chim. Acta* 309, 123–136.

(46) Nicholson, T., Cook, J., Davison, A., Rose, D. J., Maresca, K. P., Zubieta, J. A., and Jones, A. J. (1996) The synthesis and characterization of $[\text{MCl}_3(\text{N}=\text{NC}_5\text{H}_4\text{NH})(\text{HN}=\text{NC}_5\text{H}_4\text{N})]$ from $[\text{MO}_4]^-$ (where M = Re, Tc) organodiazenido, organodiazene-chelate complexes. The X-ray structure of $[\text{ReCl}_3(\text{N}=\text{NC}_5\text{H}_4\text{NH})(\text{HN}=\text{NC}_5\text{H}_4\text{N})]$. *Inorg. Chim. Acta* 252, 421–426.

(47) Nicholson, T., Cook, J., Davison, A., Rose, D. J., Maresca, K. P., Zubieta, J. A., and Jones, A. J. (1996) The synthesis, characterization and X-ray crystal structure of the rhenium organodiazenido, organodiazene complex of $[\text{ReCl}_2(\text{PPh}_3)(\text{N}=\text{NC}_5\text{H}_4\text{N})(\text{HN}=\text{NC}_5\text{H}_4\text{N})]$. *Inorg. Chim. Acta* 252, 427–430.

(48) Archer, C. M., Dilworth, J. R., Jobanputra, P., Thompson, R. M., McPartlin, M., Povey, D. C., Smith, G. W., and Kelly, J. D. (1990) Development of new technetium cores containing technetium-nitrogen multiple bonds. Synthesis and characterization of some diazenido-, hydrazido- and imido-complexes of technetium. *Polyhedron* 9, 1497–1502.

(49) Dilworth, J. R., Jobanputra, P., Thompson, R. M., Archer, C. M., Povey, D. C., Kelly, J. D., and Hiller, W. (1992) Crystal structure of a diazenido-dithiocarbamate complex of technetium, $[\text{Tc}(\text{NNC}_6\text{H}_4\text{Cl})((\text{CH}_3)_2\text{NCS}_2)_2(\text{PPh}_3)]$. *Z. Naturforsch.* 46, 449–452.

(50) Archer, C. M., Dilworth, J. R., Jobanputra, P., Thompson, R. M., McPartin, M., and Hiller, W. (1993) Technetium diazenido complexes. Part 1. Synthesis and structures of $[\text{TcCl}(\text{NNC}_6\text{H}_4\text{Cl})_2(\text{PPh}_3)_2]$ and $[\text{TcCl}(\text{NNPh})(\text{Ph}_2\text{PCH}_2\text{CH}_2\text{PPh}_2)_2][\text{PF}_6]\cdot\text{H}_2\text{O}$. *J. Chem. Soc., Dalton Trans.*, 897–904.

(51) Dilworth, J. R., Jobanputra, P., Thompson, R. M., Povey, D. C., Archer, C. M., and Kelly, J. D. (1994) Technetium diazenido complexes. Part 2. Substitution chemistry of structures of $[\text{TcCl}(\text{NNC}_6\text{H}_4\text{Cl})_2(\text{PPh}_3)_2]$ and the synthesis of technetium diazenido-complexes directly from $[\text{NH}_4][\text{TCO}_4]$. *J. Chem. Soc., Dalton Trans.*, 1251–1256.